

A Madelung Fluid Based Density Gradient Model for Large Barrier Tunneling Calculations

Venkat Narayanan and Edwin C. Kan

School of Electrical and Computer Engineering, Cornell University, Ithaca, NY 14853. Email: kan@ece.cornell.edu

Abstract

A modified density gradient model is derived for the carrier density inside a large potential barrier from the Madelung-Bohm fluid theory of quantum mechanics (QM) and the WKB approximation. The derived model is used with simple additional assumptions on the nature of the inversion layer and dissipationless transport, and shows an excellent match to experimental tunneling current data. Though the present derivation is one-dimensional, the model shows promise for generalization to 2-D and 3-D.

Introduction

Much effort has been expended towards developing computationally efficient transport models that can incorporate quantum effects. Macroscopic models based on the density gradient method [1] and the effective potential method [2] are frequently used for treating static quantum effects, such as inversion layer quantization and confinement. Of these, the effective potential method has been shown inadequate for modeling tunneling transport [3]. Though there is earlier work [4] that applies the density gradient method for treating tunneling across the barrier, the form of the equations themselves are rather unclear, owing to the fact that the method is derived from a small perturbation expansion for the Wigner function in equilibrium which diverges completely in the presence of a large barrier potential. In this paper, we remedy this shortcoming and provide a transparent derivation of a modified density gradient theory that is explicitly applicable for transport under a large potential barrier (abrupt or otherwise).

In the first section we discuss the Madelung-Bohm equations and obtain an equation obeyed by the carrier density inside a potential barrier by explicitly considering the functional forms derived in different cases. We then proceed to outline the tunneling current formulation and then present a comparison of the formulation to experimental results.

Madelung Fluid Form of the Schrödinger equation

The Schrödinger equation for a carrier system confined in an arbitrarily large box (zero flux), can be written in Madelung-Böhm form as [5],

$$[E(i) - V(x)] + \frac{\hbar^2}{2m} \frac{\nabla^2 \sqrt{P_{E(i)}}}{\sqrt{P_{E(i)}}} = 0 \quad (1)$$

The quantity P_i is the probability density, i.e. the density of a carrier in the "pure" state i , while $E(i)$ is the corresponding energy eigenvalue. P_i is of course, given by the usual relation,

$$P_i(x) = \Psi_i^*(x) \Psi_i(x) \quad (2)$$

Carriers Density Inside a Large Potential Barrier

We are interested in determining the form of the total carrier density in the mixed state (i.e. the ensemble) inside a potential barrier. The total carrier density for a carrier system can be written in terms of the eigenfunctions $\{\Psi_i\}$ of the Schrödinger equation as,

$$n(x) = n_0 \sum_i f[E(i)] \Psi_{E(i)}^*(x) \Psi_{E(i)}(x) \quad (3)$$

where, $f(E)$ is the distribution function in energy (Boltzmann or the Fermi distribution function for the degenerate and non-degenerate cases respectively) and n_0 is a suitable normalization constant obtained from a sum over all states. For the case where we have a continuous spectrum parameterized by a wavevector k , we can write the density using an integral version of (2) as,

$$n(x) = n_0 \int_0^\infty dk. f[E(k)] \Psi_k^*(x) \Psi_k(x) \quad (4)$$

In order to evaluate analytically the density in (2) inside the barrier, we can consider three different cases – that of simple potential barrier at flat band conditions, a nearly carrier system, and a confining potential on one side of the barrier shown respectively in Figs 1a, 1b and 1c, respectively.

In the first case the Schrödinger equation can be exactly solved for the scattering state basis [6], while in the other two cases, one can use the WKB approximation to obtain the wavefunctions inside the barrier. Since the latter case is quite general and subsumes the first we will present this in detail.

We can write the evanescent mode wavefunctions inside the barrier using the WKB approximation as

$$\Psi_E(x) = \frac{C}{\sqrt{p(x)}} \exp\left(-\frac{1}{\hbar} \int_0^x p(x) dx\right) \quad (5)$$

$$p(x) = \sqrt{2m(E_b + V_{sm}(x) - E)}$$

In the above, E_b is the barrier height (assumed to be large compared to the thermal energy $k_B T$) and V_{sm} is the smooth self-consistent potential. E and $p(x)$ are the energy of the state and the classical momentum respectively.

For the sake of convenience we define a wavevector corresponding to the barrier height as,

$$E_b = \frac{\hbar^2 k_b^2}{2m} \quad (6)$$

We also define the thermal wavelength, λ_{th}

$$\lambda_{th} = \sqrt{\frac{\hbar^2}{2mk_b T}} \quad (7)$$

Writing the momentum in terms of the wavevector k using the de-Broglie relation, we can write the above for a large barrier to a very good approximation as,

$$\begin{aligned} \Psi_E(x) &= C_1 \exp\left(-k_b \int_0^x \sqrt{1 + \frac{V_{sm}(x) - E}{E_b}} dx - \frac{1}{4} \ln\left(1 + \frac{V_{sm}(x) - E}{E_b}\right)\right) \\ &\approx C_1 \exp\left(-k_b x + \frac{k^2 x}{2k_b} - k_b \int_0^x \frac{V_{sm}(x)}{2E_b} dx + \frac{k^2}{4k_b^2} - \frac{V_{sm}(x)}{4E_b}\right) \end{aligned} \quad (8)$$

We note formally that the probability density $P_E(x)$ corresponding to the above wavefunction satisfies (1) inside the barrier, which can be solved to yield (6) if the boundary conditions on the probability density on either side of the barrier were known.

Computing the density inside the barrier using (4) and the Boltzmann distribution function with the above expression for the wavefunction yields [7],

$$\begin{aligned} n(x) &= n_0 \frac{\exp\left(-2k_b x - 2k_b \int_0^x \frac{V_{sm}(x)}{4E_b} dx - \frac{V_{sm}(x)}{2E_b}\right)}{\sqrt{1 - \frac{x}{\lambda_{th} \sqrt{\beta E_b}} - \frac{1}{2\beta E_b}}} \quad (9) \\ &= n_0 \exp\left(-2k_b \left(x + \int_0^x \frac{V_{sm}(x)}{4E_b} dx\right) + \frac{x}{\lambda_{th} \sqrt{\beta E_b}} + \frac{1}{2\beta E_b} - \frac{V_{sm}(x)}{2E_b}\right) \end{aligned}$$

It is immediately seen on comparing (7) with (6) that the density inside the barrier obeys the following relation

$$n(x) \propto P_{\langle E \rangle}(x) \quad (10)$$

with the average energy obtained by averaging over the eigen-energies of the one-dimensional Schrodinger equation.

$$\langle E \rangle = \sum_i E(i) f[E(i)] \quad (11)$$

In this particular case, since Boltzmann statistics was used to demonstrate the idea the average energy is the kinetic energy corresponding to a classical electron gas in one direction, i.e.

$$\langle E \rangle = \frac{k_b T}{2} \quad (12)$$

the average energy due to motion of carriers towards the oxide interface.

Thus the functional form of the *total* (mixed-state) density inside the barrier is the same as an appropriate pure-state probability density at an average energy $kT/2$ and therefore it satisfies the differential equation,

$$[\langle E \rangle - V(x)] + \frac{\hbar^2}{2m} \frac{\nabla^2 \sqrt{n}}{\sqrt{n}} = 0 \quad (13)$$

It should be noted here, that unlike the usual derivation of density-gradient theory which starts from the free electron Wigner function [1], the presence and largeness of the barrier are directly incorporated into the derivation of Equation (12), by explicitly considering the density function inside the barrier.

Bound states and Fermi-Dirac statistics

Although the derivation in the previous section considered a continuous spectrum and Boltzmann statistics for demonstration, the situation can be readily extended to degenerate carrier gases using Fermi-Dirac statistics and for the case of carriers in bound states leaking through a barrier (Fig. 1c). In this case one will need to employ the discrete sum (3) in addition to (4) to evaluate the density inside the barrier [7].

For large potential barriers with quantized states on one side (similar to a MOSFET in the inversion regime) the average energy in Equation (13) will only be determined by the quantized states outside the barrier. The evanescent modes inside the barrier are a small perturbation and do not contribute significantly to the average energy. The increased average energy due to quantization outside the barrier results in higher penetration into the barrier.

Tunneling Current Formulation

Now that the equation for the density inside the barrier is unambiguously derived we can proceed to a calculation of the direct tunneling gate current of a MOSFET for demonstration [9]. We follow broadly the procedure adopted in [4] for elastic tunneling by separating the carrier populations emitted from the two contacts (in this case from the substrate and the gate respectively). This procedure is valid since we do not normally consider scattering processes that can mix the

injected carriers from the two contacts while calculating the tunneling current through a barrier.

Each of the two populations injected into the barrier from the contacts individually obeys (4) that can be solved to yield the density variation inside the barrier. There are two boundary conditions required to solve Equation (13) for carriers injected from each of the two contacts. The first boundary condition is obtained from the upstream (injecting) contact and is a simple Dirichlet condition depending on the density of carriers at the oxide-semiconductor interface. In this case we use a relation derived in [10], which shows that the carrier density is suppressed by a factor of βE_b from the classical case near a large barrier.

$$n_1 = \frac{N_c F_{1/2}(\eta_c)}{\beta E_b}, \quad \eta_c = \frac{E_c - E_F}{k_B T} \quad (14)$$

where n_1 is the density of the population injected into the barrier from the substrate at inversion.

The two populations differ in their Fermi levels, which they retain from the originating contact, and thus in the boundary conditions imposed on the respective differential equation (Fig. 2.). The condition is not unlike a p-n junction diode, where electrons and hole quasi-Fermi levels are constant across a depletion region because of a lack of recombination. Once across the depletion region the Fermi levels are equalized by recombination. For the case of two carriers the driving force for the equalization of Fermi levels is recombination. For a single carrier, emitted from two different contacts with different Fermi levels the driving force is scattering and in the absence of these the injected populations retain the Fermi level of the originating contact until they suffer inelastic scattering processes downstream at the other contact.

The *virtual anode* boundary conditions at the downstream contact [4] are used for the second boundary condition to solve (13).

$$\left. \frac{\partial n_1}{\partial x} \right|_{x=l_{oc}} \approx 0 \quad (15)$$

For the barrier thicknesses that are of interest (> 0.5 nm) the above boundary condition yields negligible error in the carrier density.

The current is calculated using the relation,

$$J_n = q \gamma_2 n_1 \quad (16)$$

where γ_2 is a recombination velocity at the downstream contact. This determines the rate at which carriers are absorbed into the downstream contact by inelastic scattering processes. Once again the p-n junction diode analogy is apt. In a p-n junction diode the current is determined by the rate of recombination of electrons (holes) at the p (n) type region as minority carriers. In the tunneling example for single carriers the current is determined by the inelastic scattering processes that relax the carriers back to the Fermi level of the downstream contact. In the absence of any detailed models for these processes we use an aggregate fitting parameter γ to model it.

The model requires an input in terms of the average energy of carriers entering the barrier from each contact in Equation (13). This depends on the detailed potential profile at the upstream contact, but for simplicity the van Dort model [8], which assumes a triangular well is used in this work. In particular we have used,

$$\langle E \rangle \approx E_c + 1.857 \left(\frac{q\hbar}{\sqrt{m_{Si}}} F_{surf} \right)^{2/3} \quad (17)$$

where E_c is the conduction band edge as the average energy of carriers in the Equation (13). This can of course, be further refined in the spirit of the macroscopic treatment of the inversion layer.

Numerical Results

Figure 3 shows the injected carrier densities from each contact over a 1.5nm oxide barrier with an applied bias of 2V. Notice that n_1 and n_2 represent the QM densities under the tunneling conditions in the classically forbidden oxide bandgap. If the Fermi levels on the two sides of the barrier are equal, then the resulting flux from each will cancel out exactly. Figure 4 shows an excellent match for the model to experimental data over a range of applied biases and oxide thickness.

The applicability of the above method only hinges on the WKB assumption for the functional form of the evanescent modes inside the barrier and can hence be applied for the F-N tunneling regime simply by changing the integration limits for (4). All other corrections such as effective mass variation can also be readily applied.

Conclusions

We have presented a modified density gradient model based on the Madelung-Bohm fluid theory of QM including all large-barrier information *without incurring small perturbation equilibrium assumptions* on the Wigner function. The presentation here completely circumvents all the usual problems of abrupt variation of the potential, as well as the

largeness of the potential usually encountered in derivations of density-gradient theory. The formalism is promising to be directly incorporated in device simulation.

References

- [1] M.G. Ancona et. al, , *Phys. Rev. B*, vol. 39, no. 13, May 1989.
- [2] D.K. Ferry, *IEDM Tech. Dig.*, pp. 287-290, December 2000.
- [3] D.K. Ferry, *Journal of Comp. Elec.*, Kluwer Publishers, January 2002.
- [4] M.G. Ancona, *Phys. Rev. B*, vol. 42, no. 2, pp. 1222-1233 July 1990
- [5] D. Bohm, *Phys. Rev.* , vol. 85, no. 2, pp. 166-179, January 1952.
- [6] A. Kriman et. al, *Phys. Rev. B*, vol. 36, no. 11, pp. 5953-5960, October 1987
- [7] V. Narayanan, *Ph.D Thesis*, Cornell University, May 2006.
- [8] M. J. van Dort et. al, *Solid State Electronics*, vol. 32, no. 3, pp. 411-414, 1994
- [9] N. Yang, et. al, *IEEE Trans. Electron Dev.*, vol. ED-46, no. 7, pp. 1464-1472, July 1999.
- [10] V. Narayanan, et. al, *Journal of Comp. Elec.*, Kluwer Publishers, pp. 435-438, January 2005.

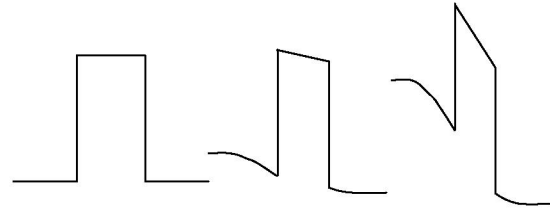


Fig. 1 a) Simple potential barrier at flat band, b) Large potential barrier without a confining well c) Large potential barrier with a confining potential well

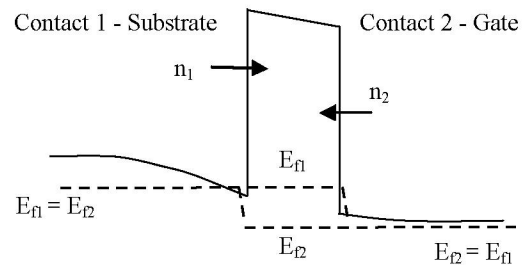


Fig. 2 Variation of the chemical potentials, for electrons only, injected from the two “contacts” 1 and 2. The equalization of the chemical potentials occurs due to thermalization processes in the “downstream” contacts and the rate of recombination directly yields the current

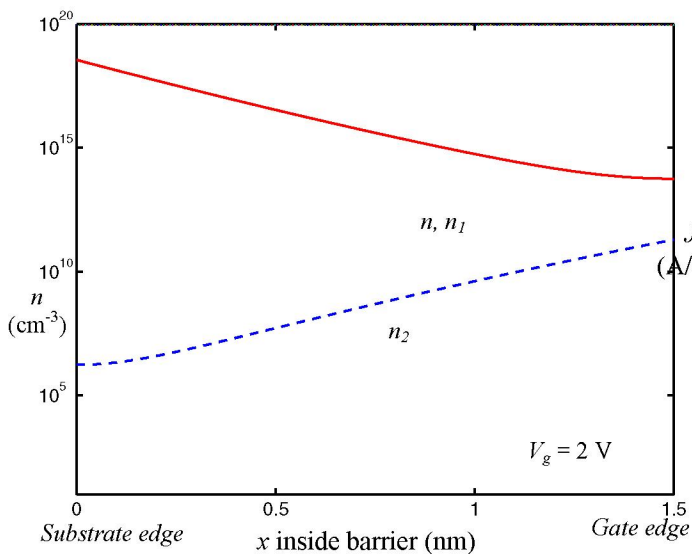


Fig. 3. The total density n , and the individual injected densities n_1 and n_2 from the solution of (4) with the Poisson equation. The high tail of n_1 is responsible for the large tunneling current in Fig. 4.

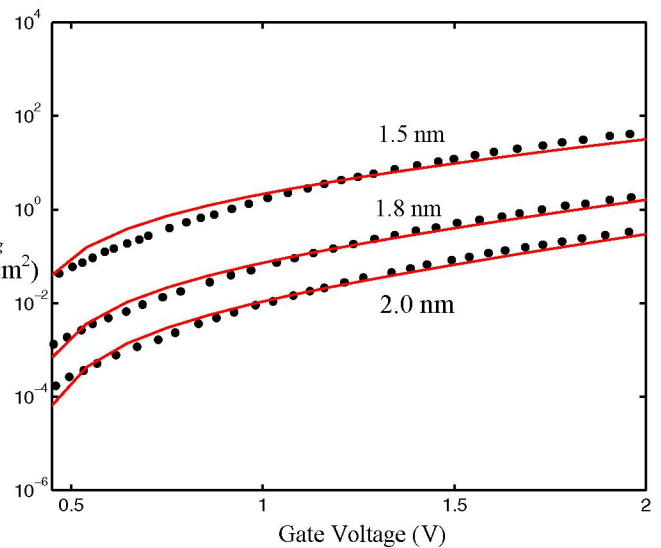


Fig. 4. Direct tunneling current densities, calculated including a simple triangular well quantization condition for the average energy, compared to data from [9]. Solid lines are the simulation results while the dots indicate data points. The oxide thicknesses are indicated next to the plots.